Available online at www.sciencedirect.com
ScienceDirect
Journal of Organometallic Chemistry 692 (2007) 2519–2528
Journal of Organometallic Chemistry
www.elsevier.com/locate/jorganchem

Hemilabile orthometallated acetals: Synthesis, spectroscopic characterization and crystal and molecular structures of $[RuCl\{\eta^2\text{-}C,O\text{-}C_6H_4\text{-}2\text{-}CH(O_2C_2H_4)\}(CO)(PPh_3)_2]$ and $[HgBr\{\eta^2\text{-}C,O\text{-}C_6H_4\text{-}2\text{-}CH(O_2C_2H_4)\}]$

Rosalyn J. Evans [a], Kevin R. Flower [a,*], Laura G. Leal [a], Patrick J. O'Malley [a], Claudia Mangold [a], Robin G. Pritchard [a], John E. Warren [b]

[a] School of Chemistry, University of Manchester, Oxford Road, Manchester M13 9PL, UK
[b] CCLRC Daresbury Laboratory Daresbury, Warrington, Cheshire WA4 4NS, UK

Received 18 January 2007; received in revised form 16 February 2007
Available online 24 February 2007

Abstract

Treatment of $[RuHCl(CO)(PPh_3)_2]$ with $[Hg\{C_6H_4\text{-}2\text{-}H(O_2C_2H_4)\}_2]$ (**1**) in refluxing toluene affords $[RuCl\{\eta^2\text{-}C,O\text{-}C_6H_4\text{-}2\text{-}CH(O_2C_2H_4)\}(CO)(PPh_3)_2]$ (**2a**). Compound **2a** reacts with $Ag[BF_4]$ followed by NaX (X = Br, I, F) to give $[RuX\{\eta^2\text{-}C,O\text{-}C_6H_4\text{-}2\text{-}CH(O_2C_2H_4)\}(CO)(PPh_3)_2]$ (**2b–d**). All compounds have been characterized by elemental analysis (C and H), IR, ^1H, $^{13}C\text{–}\{^1H\}$ and $^{31}P\text{–}\{^1H\}$ NMR spectroscopy. A crystallographic study of **2a** shows the presence one pair of enantiomers and one pair of diastereoisomers in the asymmetric unit. Theoretical calculations (B3LYP using the LanL2DZ basis set) on the model compounds $[RuCl(CH_3)(EH_2)(CO)(PH_3)_2]$ (E = O, S) (**3a**,**b**) show that for **3a** a planar geometry at the OH_2 ligand and for **3b** a pyramidal structure at SH_2 is favoured. The calculated electrostatic potentials for EH_2 and the acetals $CH_2E_2C_2H_4$ (E = O, S) are used to comment on the nature of the lone pairs at the chalcogen atoms and the coordination geometries of ether and thioether ligands. The X-ray crystallographically determined molecular structure of $[BrHg(\eta^2\text{-}C,O\text{-}C_6H_4\text{-}2\text{-}CHO_2C_2H_4)]$ (**4**) is also described and model compounds studied theoretically.

Keywords: Ruthenium; Orthometallation; Acetal; Pyramidal inversion; Crystallography; Halide

1. Introduction

Recently we reported the preparation of some cycloruthenated azobenzene [1] and Schiff base [2] complexes and showed the presence of a non-conventional *cis*-push–pull effect, Chart 1, that complements the normal *cis*-push–pull effect observed between a halide and carbonyl ligand [3]. As an extension to this study we were interested in synthesising molecules in which the non-conventional *cis*-push–pull effect could not be effected by the cyclometallated ligand and hence see if the relative magnitude of each effect be deciphered.

Several years ago we described [4] the synthesis of the diorganomercurial $Hg\{o\text{-}C_6H_4\text{-}2\text{-}CH(O_2C_2H_4)\}_2$ and considered it to be an ideal candidate to act as a transfer reagent for the hemilabile ligand $\{o\text{-}C_6H_4\text{-}2\text{-}CH(O_2C_2H_4)\}_2$ as it would not transmit the secondary *cis*-push–pull effect observed in the related cyclometallated imine and azo-containing systems. It was also anticipated that the acetal ring would undergo an acetal-ring rotation similar to that previously observed in rhenium carbonyl halide complexes containing {pyridine-1,3-dioxan-2-yl}-based ligands and therefore provide more information on this fluxional process [5]. A better understanding of the nature of these

* Corresponding author. Tel.: +44 0 1613064538; fax: +44 0 1612754598.
E-mail address: k.r.flower@manchester.ac.uk (K.R. Flower).

0022-328X/$ - see front matter © 2007 Elsevier B.V. All rights reserved.
doi:10.1016/j.jorganchem.2007.02.029

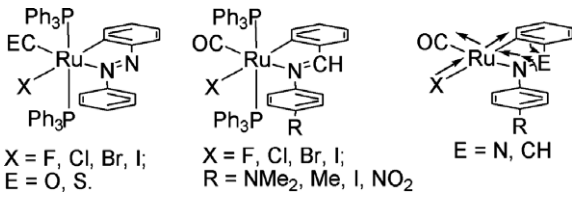

Chart 1. Non-conventional *cis*-push–pull effect facilitated by cylometallated ligands.

fluxional processes is useful in understanding the dynamics of this type of ligand and the development of new hemilabile ligand sets for use in homogeneous catalysis [6]. During the course of this work Vicente et al. reported the preparation of some analogous orthomercuriated arylacetals and their utility as transfer reagents in the preparation of some orthopalladated arylacetal complexes [7]. The number of other examples of cyclometallated (η^2-*C*,*O* coordinated) aryl acetals is limited [8].

Herein we describe the synthesis and characterization of the cycloruthenated acetal containing complexes $[RuX\{\eta^2\text{-}C,O\text{-}C_6H_4\text{-}2\text{-}CH(O_2C_2H_4)\}(CO)(PPh_3)_2]$ (**2a**–**d**) (X = Cl, Br, I, F); the fluxional nature of the acetal ring; the presence of diastereoisomers in the crystal structure of **2a** which are a result of pseudorotation of the five-membered acetal ring; and why pyramidal inversion is readily observed in thioether-containing complexes but not analogous ether-containing complexes.

2. Results and discussion

2.1. Syntheses and characterization of $[RuX(CO)\{\eta^2\text{-}C, O\text{-}C_6H_4\text{-}2\text{-}CH(O_2C_2H_4)\}(PPh_3)_2]$ (X = Cl, **2a**; Br, **2b**; I, **2c**; F, **2d**)

Compound **2a** was prepared by modification of the methodology reported by Roper and Wright [9], and compounds **2b**–**d** were prepared by a Ag^+ mediated halogen exchange reaction, Scheme 1.

All of the new compounds **2a**–**d** were characterized by microanalysis (C, H), and IR spectroscopy Table 1, ^1H, $^{31}P\{^1H\}$ NMR spectroscopy Table 2 and $^{13}C\{^1H\}$ NMR spectroscopy Table 3. Compound **2a** was also characterized by a single crystal X-ray diffraction study, see Table 4 for data collection and processing parameters and the Section 4 for additional comments on the structure solution. PLUTON [10] representations of the crystallographically independent molecules are presented in Fig. 1 showing the numbering scheme and selected bond lengths (Å) and angles (°).

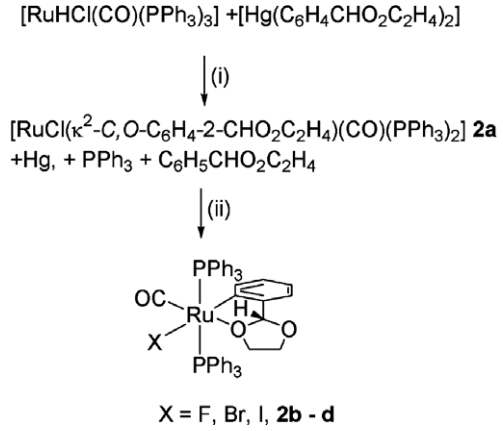

Scheme 1. Synthetic scheme for the preparation of **2a**–**d**. (i) $C_6H_5CH_3$, reflux, 6h; (ii) $Ag[BF_4]$, $CH_2Cl_2/(CH_3)_2CO$; NaX, (X = F, Br, I).

Each of the independent molecules is conveniently described as a slightly distorted octahedral with the two PPh_3 ligands mutually trans and axial with the orthoruthenated-2-phenylacetal, carbonyl and chloride ligands in the equatorial plane. The four molecules can be considered as one pair of enantiomers where the sum of the angles about the coordinated acetal oxygen is 359.8° and one pair of diasteroisomers where the sum of the angles about the coordinated oxygen atom is 354.1°. These coordination geometries at oxygen can be considered as intermediates in the classical pyramidal inversion process [11], frequently observed in related sulfur systems, and often investigated by VT NMR [12]. A search of the CCDC [13] shows that a planar oxygen environment is dominant in metal ether complexes and on careful examination of relative ligand orientations in these complexes there is no evidence that oxygen planarity results from π-effects. For related thioether-containing complexes pyramidal geometry at sulfur is, as expected, normal. For example Vicente et al. have recently reported the solid state structure of the cyclopalladated thioacetal-containing complex $[PdCl\{\eta^2\text{-}C,S\text{-}C_6H_3\text{-}2,5\text{-}(CHS_2C_2H_4)\}(PPh_3)]$ and the thioacetal ligand is pyramidal at sulfur [7].

In an attempt to rationalize why the ether-containing complexes appear to prefer planar and the thioether-containing complexes pyramidal geometries at the coordinated chalcogen atom theoretical calculations (B3LYP using the LanL2DZ basis set) [14] were carried out on the model compounds $[RuCl(CH_3)(EH_2)(CO)(PH_3)_2]$ (E = O, S) (**3a**,**b**), Figs. 2 and 3 [15]. See Supplementary material for calculated bond lengths (Å) and angles (°). For **3a** the structural minimum contains planar oxygen and this minimized structure sits at the bottom of a single potential well. Conversely, for **3b** pyramidal geometry at sulfur is calculated to be the energetic minimum. A complex containing planar sulfur is found to represent the transition state geometry of a classical double potential well representation of a pyramidal inversion process with a calculated activation barrier of 44 kJ mol^{-1}. Recent calculations carried out on the $[M(OH_2)_2]^+$ cations (M = Ag, Au, Cd, Hg) likewise predict a single potential well for the coordinated aquo-ligand [16]. Structural minimization at the B3LYP LanL2DZ level for H_2E and $HCE_2C_2H_4$ (E = O, S) has also been carried out and electrostatic plots (−30 kcal mol^{-1}) are presented in Fig. 4. They show for E = O the electron density has a banana-like appearance with the maximal electron density found to be located in the OR_2 plane. This suggests that planar coordination is most likely in aquo and

Table 1
Physical, analytical[a], and infrared data[b] for **2a–d**

Compound	Color	Yield (%)	Microanalytical data (%). Calc in parentheses			IR ν(CO) cm^{-1}
			Mp (°C)	C	H	
2a [RuCl(CO){η^2-$C_6H_4CH(O_2C_2H_4)$}$(PPh_3)_2$]	White	87	224	66.1 (65.9)	4.9 (4.7)	1921
2b [RuBr(CO){η^2-$C_6H_4CH(O_2C_2H_4)$}$(PPh_3)_2$]	White	94	219	62.7 (62.6)	4.5 (4.5)	1930
2c [RuI(CO){η^2-$C_6H_4CH(O_2C_2H_4)$}$(PPh_3)_2$]	White	96	217	59.3 (59.4)	4.1 (4.2)	1930
2d [RuF(CO){η^2-$C_6H_4CH(O_2C_2H_4)$}$(PPh_3)_2$]	White	68	212	66.5 (67.2)	4.5 (4.8)	1914
4 [HgBr{η^2-C_6H_4-2-$CH(O_2C_2H_4)$}]	White	75	187	25.2 (25.2)	2.1 (2.1)	

[a] Calculated values in parentheses.
[b] Spectra recorded as nujol mulls between KBr plates all bands strong.

Table 2
$^{31}P\{^1H\}$ NMR[a] and proton data[b] for compounds **2a–d**

Compd	^{31}P (δ)	^1H (δ)
2a	32.6 (AB $J_{PP} = 338$)	7.75–7.12 (m, 30H aryl-H); 6.74 (d, $J_{HH} = 7.2$, 1H, aryl-H); 6.62 (t, $J_{HH} = 7.2$, 1H, aryl-H); 6.00 (t, $J_{HH} = 7.5$, 1H, aryl-H); 5.78 (d, $J_{HH} = 7.9$, 1H, aryl-H); 4.82 (s, 1H, CH); 3.66 (br s, 1H, OCH_2); 3.46 (br s, 1H, OCH_2); 3.30 (br s, 1H, OCH_2); 2.62 (br s, 1H, OCH_2)
2b	32.5 (AB, $J_{PP} = 301$)	7.60–7.10 (m, 30H aryl-H); 6.70 (d, $J_{HH} = 7.5$, 1H, aryl-H); 6.59 (t, $J_{HH} = 7.5$, 1H, aryl-H); 5.99 (t, $J_{HH} = 7.6$, 1H, aryl-H); 5.78 (d, $J_{HH} = 7.8$, 1H, aryl-H); 4.66 (s, 1H, CH); 3.40 (br s, 1H, OCH_2); 3.33 (br s, 1H, OCH_2); 3.17 (br s, 1H, OCH_2); 2.69 (br s, 1H, OCH_2)
2c	31.9 (s)	7.60–7.10 (m, 30H, aryl-H); 6.70 (d, $J_{HH} = 7.5$, 1H, aryl-H); 6.23 (t, $J_{HH} = 7.6$, 1H, aryl-H); 6.06 (t, $J_{HH} = 7.1$, 1H, aryl-H); 5.90 (d, $J_{HH} = 7.8$, 1H, aryl-H); 4.51 (s, 1H, CH); 3.50 (br s, 1H, OCH_2); 3.30 (br s, 1H, OCH_2); 3.20 (br s, 1H, OCH_2); 2.85 (br s, 1H, OCH_2)
2d	33.0 (AB, $J_{PP} = 327$, $J_{PF} = 14.9$)	7.70–7.10 (m, 30H, aryl-H); 6.70 (d, $J_{HH} = 7.6$, 1H, aryl-H); 6.53 (t, $J_{HH} = 7.5$, 1H, aryl-H); 6.00 (t, $J_{HH} = 7.6$, 1H, aryl-H); 5.83 (d, $J_{HH} = 7.6$, 1H, aryl-H); 5.04 (s, 1H, CH); 3.75–3.25 (br m, 4H, OCH_2)
4		7.41–7.25 (m, 4H, aryl-H); 5.65 (s, $J_{HgH} = 84.4$, 1H, CH); 4.27–3.94 (m, 4H, CH_2)

[a] Spectra recorded (162.6 MHz) in $CDCl_3$ at 296 K; coupling constants (J) Hz, s = singlet, d = doublet, t = triplet, m = multiplet, AB = AB quartet.
[b] Spectra recorded (200 MHz) in $CDCl_3$ at 296 K.

Table 3
$^{13}C\{^1H\}$ NMR data[a] for compounds **2a–d**

Compd	^{13}C (δ)
2a	206.6 (t, $J_{PC} = 17.4$, CO); 166.0 (t, $J_{PC} = 9.6$, RuC); 140.0; 136.0; 134.4; 133.5 (d, $J_{PC} = 43.5$); 132.4 (d, $J_{PC} = 64.4$); 129.5; 129.1; 128.7; 121.7; 120.2; 110.2; 64.8; 63.7
2b	206.7 (t, $J_{PC} = 16.4$ CO); 166.0 (t, $J_{PC} = 10.6$, RuC); 140.4; 136.0; 134.3; 133.5 (d, $J_{PC} = 34.8$); 132.3 (d, $J_{PC} = 61.4$); 129.4; 129.3; 129.1; 127.6; 121.6; 120.5; 110.2; 64.8; 63.9
2c	207.3 (br s); 166.0 (br s); 140.8; 136.0; 135; 133.7 (br s); 132.7 (br s); 129.5; 129.4; 129.1; 127.6; 121.6; 120.7; 110.3; 65.5; 64.4
2d	206.7 (br m); 166 (br m); 140.1; 136.0; 134.4; 133.9; 133.6; 133.0; 129.1; 128.7; 128.5; 127.8; 127.6; 121.7; 120.2; 110.2; 64.8; 63.9
4	151.1; 141.0; 130.9; 129.2; 130.4; 137.0; 104.2; 65.4

[a] Spectra recorded (100.55 MHz) in $CDCl_3$ at 296 K; all resonances singlets unless otherwise stated; coupling constants (J) Hz.

ether-containing complexes however, deformation from strict planar geometry is energetically not too costly. Whereas for E = S clear evidence of two concentrations of electron density akin to the classical bunny-ear representation of lone pairs is visible indicating a clear preference for pyramidal binding. These binding modes suggested by calculation are also consistent with the preferred binding modes found in the CCDC. It is also consistent with why pyramidal inversion is readily observable for thioether-containing complexes and not for ether-containing complexes using VT NMR techniques: the transition state for the complexed ether oxygen inversion is the energetic minimum rather than the energetic maximum.

It is well known and documented that five-membered rings are conformationally flexible [17] and that the observed puckering can rotate easily around the ring through 10 C_2 and 10 C_s forms without the interference of significant enthalpy barriers. This pseudorotation has a maximum torsion angle θ_m and a phase angle of pseudorotation P. Each can be readily calculated [17b] and utilising the crystallographic data obtained for **2a** the calculated value of θ_m for each acetal ring is 43.36, 42.93, 41.22, 41.04

Table 4
X-ray crystallographic data for **2a** and **4**

Compound	**2a**	**4**
Empirical formula	$C_{188}H_{166}Cl_4O_{13}P_8Ru_4$	$C_9H_9BrHgO_2$
Formula weight	3427.05	429.66
Temperature (K)	120(2)	200(2)
Wavelength (Å)	0.68630 (Synchrotron)	0.71073 (Kappa CCD)
Crystal system	Monoclinic	Monoclinic
Space group	$P121/c1$	$P2_1/n$
Unit cell dimensions		
a (Å)	10.7814(13)	9.0456(4)
b (Å)	36.167(4)	4.3690(2)
c (Å)	41.839(5)	25.5155(14)
β (°)	90.109(2)	90.927(2)
Volume (Å^3)	16314(3)	1008.25(8)
Z	4	4
D_{calc} (Mg/m^3)	1.395	2.831
Absorption coefficient (mm^{-1})	0.487	19.191
$F(000)$	7048	776
Crystal size (mm)	$0.08 \times 0.02 \times 0.01$	$0.20 \times 0.06 \times 0.04$
θ (°)	2.82–26.45	3.31–25.25
h,k,l	$-13 \leqslant h \leqslant 13$, $-46 \leqslant k \leqslant 46$, $-48 \leqslant l \leqslant 54$	$0 \leqslant h \leqslant 10$, $0 \leqslant k \leqslant 5$, $-30 \leqslant l \leqslant 30$
Reflections collected	124375	1796
Independent reflections [$R_{(int)}$]	36753 [0.0802]	1796 [0.0000]
Completeness to θ (%)	98.6	98.7
Absorption correction	None	Semi-empirical from equivalents
Maximum and minimum transmission	0.9951 and 0.9621	0.5140 and 0.1140
Refinement method	Full-matrix-block least-squares on F^2	Full-matrix least-squares on F^2
Data/restraints/parameters	36753/0/1973	1796/0/119
Final R indices [$I > 2\sigma(I)$]	$R_1 = 0.0637$, $wR_2 = 0.1489$	$R_1 = 0.0421$, $wR_2 = 0.0981$
R indices (all data)	$R_1 = 0.0945$, $wR_2 = 0.1641$	$R_1 = 0.0593$, $wR_2 = 0.1111$
Goodness-of-fit on F^2	1.026	1.060
Extinction coefficient	0.00132(8)	0.0008(3)
Largest difference in peak and hole (e Å^{-3})	1.332 and −1.452	1.977 and −1.850

(°) respectively with the phase angle P for each ring being 162.7, 92.0, (close to theoretical planar angles of 162 and 90 °) and 137.1, 140.6 (close to the C_2 ring angle of 144 °). This pseudorotation also clearly affects the coordination geometry at the complexed oxygen atom, Fig. 1, in each of the independent molecules in the crystal structure. Hence the presence of one pair of enantiomers, chiral only at carbon, and one pair of diasteroisomers, chiral at both carbon and oxygen. Therefore, based on data from the theoretical calculations and the nature of the pseudorotation observed in five-membered ring systems, the planar and pyramidal oxygen atoms observed in the solid state structure of **2a** are unlikely to represent trapped intermediates in the classical pyramidal inversion process rather they represent frozen intermediates on a low energy pseudorotation pathway.

Compounds **2a–d** would be expected to give an AB quartet resonance in their $^{31}P\{^1H\}$ NMR spectra when the cycloruthenated acetal ligand is coordinated as a C–O chelate, containing a planar oxygen atom. From the data presented in Table 1 compounds **2a**, **b** and **d** (which shows additional coupling to fluorine) fit this expectation (AB quartet), whereas **2c** (singlet) does not and therefore appears to be fluxional at room temperature. The fluxional process that is in operation is dechelation of the acetal oxygen with associated ring rotation about the aryl–acetal–*CH*-bond. This process causes equilibration of the *trans*-phosphine ligands and hence the appearance of a singlet resonance. It also effects inversion of the chirality at the acetal O_2CH–Ph carbon atom. Inversion at the ligated oxygen atom is also a possible fluxional process. However, this mechanism does not equilibrate the two phosphorus atoms as the acetal C*H* will always point towards the same phosphine ligand and therefore prevent resonance equilibration. Cooling a $CDCl_3$ solution of **2c** caused broadening of the spectral line consistent which is consistent with slowing down the rate of ring rotation, conversely warming of a $CDCl_3$ solution of **2a** caused broadening of the signal indicative of speeding-up the ring rotation. In neither case could enough data be collected to allow calculation of the barrier to acetal ring rotation.

The ^1H and $^{13}C–\{^1H\}$ NMR data, Tables 1 and 2, are likewise indicative of the compounds **2a–d** being fluxional. The fluxional process for **2a** was investigated by a VT ^1H NMR study in $CDCl_3$ at 400 MHz. The pertinent portions of the recorded spectra are illustrated in Fig. 5. At low temperature (233 K) the spectrum is consistent with a 'static-structure' that contains a planar-coordinated acetal oxygen atom. There is no evidence for the presence of an additional set of resonances that would be consistent with the presence of a pair of diasteroisomers that would necessarily contain pyramidally coordinated oxygen.

As the temperature is elevated above room temperature evidence for ring rotation is observed. The expected two proton resonances for each of the OCH_2 groups (proxal and distal) to the acetal CH is not attained as coalescence of one pair of signals occurs just below the boiling point of the solvent; hence the presence of only one sharp signal. The other is very broad and essentially lost in the baseline. The barrier ($\Delta G^{\ddagger}$) to ring rotation was calculated to be 62 ± 2 kJ mol^{-1} and is consistent with other acetal ring rotations [5]. Dechelation of the acetal oxygen atom offers a vacant coordination site. Attempts to trap the dechelated intermediate using the Lewis bases, CO, CNBu^t were carried out and no evidence of ligand coordination or migratory insertion observed. The non-reactivity presumably results from the acetal ring blocking access of an incoming ligand as it rotates. The acetal ring also seems quite stable with respect to hydrolysis.

The IR spectra for **2a–d** (Table 1) all show an expected strong ν(CO) band between 1914 and 1930 cm^{-1} ($\Delta\nu$(CO) = 16 cm^{-1}), with the lowest stretch being for **2d** (X = F). This is expected as the fluoride ligand is the

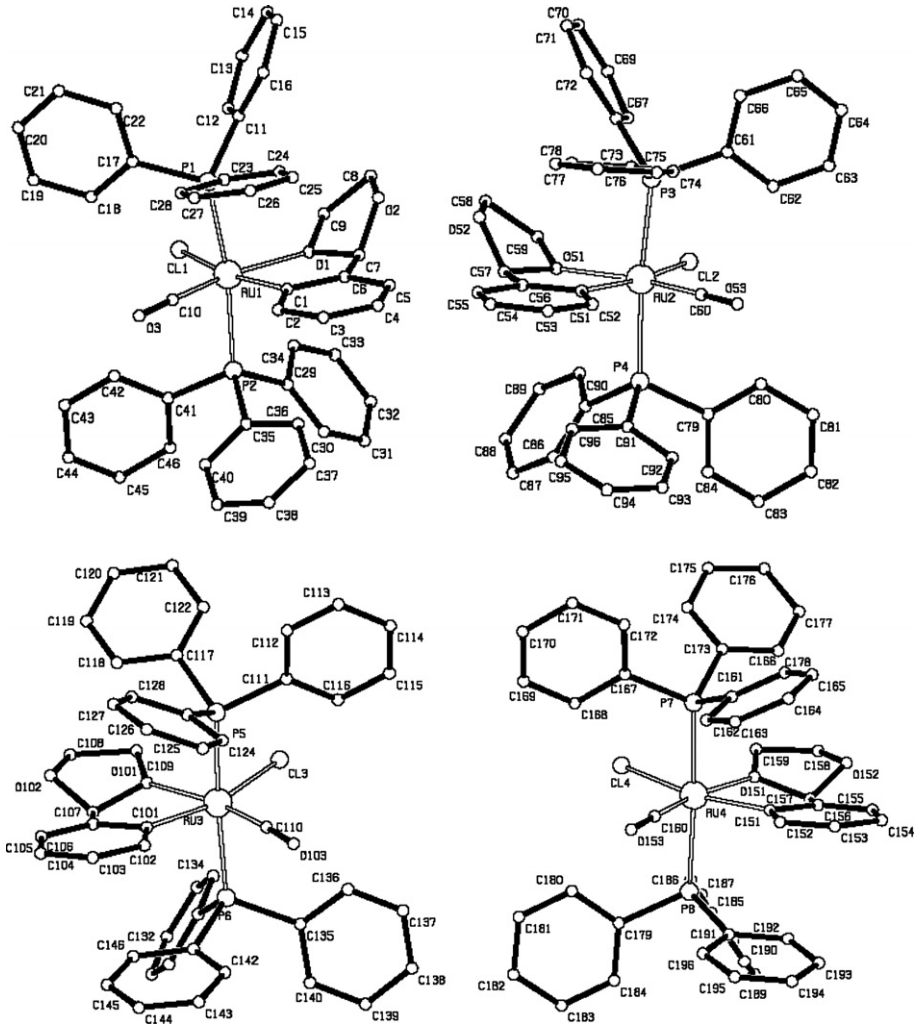

Fig. 1. PLUTON representations of the independent molecules of **2a** showing the atomic numbering scheme. Selected bond lengths (Å) and angles (°): Ru(1)–C(10) 1.794(6); Ru(1)–C(1) 2.062(6); Ru(1)–O(1) 2.222(4) Ru(1)–P(2) 2.3773(16); Ru(1)–P(1) 2.3775(16); Ru(1)–Cl(1) 2.4920(15); Ru(2)–C(60) 1.816(7); Ru(2)–C(51) 2.055(6); Ru(2)–O(51) 2.208(4); Ru(2)–Cl(2) 2.4981(16); Ru(3)–C(110) 1.782(7); Ru(3)–C(101) 2.070(6); Ru(3)–O(101) 2.198(5); Ru(3)–Cl(3) 2.5172(17); Ru(4)–C(160) 1.799(7); Ru(4)–C(151) 2.077(6); Ru(4)–O(151) 2.190(5); Ru(4)–Cl(4) 2.5148(17); C(9)–O(1)–C(7)104.3(4); C(9)–O(1)–Ru(1) 134.9(4); C(7)–O(1)–Ru(1) 115.0(3); C(59)–O(51)–C(57) 104.0(5); C(59)–O(51)–Ru(2)134.9(4); C(57)–O(51)–Ru(2)115.8(4);C(109)–O(101)–C(107) 107.9(5); C(109)–O(101)–Ru(3)139.5(4); C(107)–O(101)–Ru(3) 112.6(4); C(159)–O(151)–C(157) 107.4(5); C(159)–O(151)–Ru(4) 139.5(4); C(157)–O(151)–Ru(4) 113.1(4).

Fig. 2. SPARTAN representation of the optimized geometry of $[RuCl(CH_3)(OH_2)(CO)(PH_3)_2]$ (**3a**).

Fig. 3. SPARTAN representation of the optimized geometry of $[RuCl(CH_3)(SH_2)(CO)(PH_3)_2]$ (**3b**).

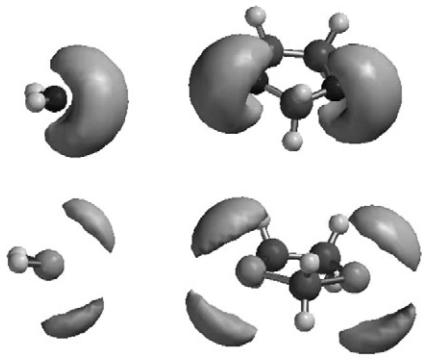

Fig. 4. Electrostatic contour plots at -30 kcal mol^{-1} for H_2O, H_2S, $CH_2O_2C_2H_4$ and $CH_2S_2C_2H_4$.

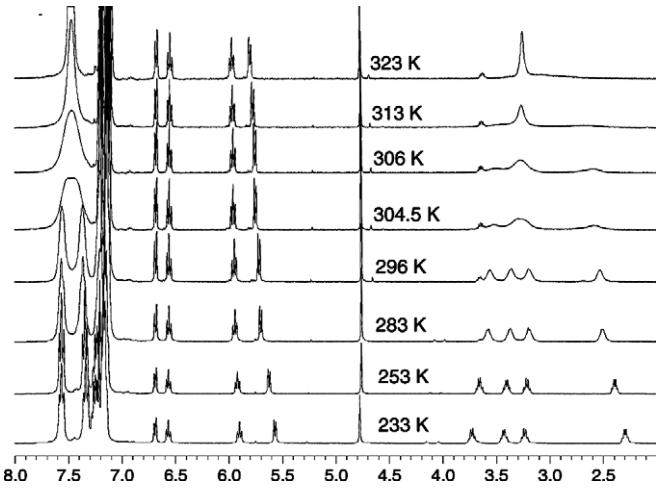

Fig. 5. VT ^{1}H NMR spectra for **2a** from 233–253 K.

strongest π-donor and has been noted previously in related work [18] and by others [19]. Recently we reported [18] the preparation of the related series of compounds [RuX(CO)-(η^2-*C*,*N*-$C_6H_4CH{=}NC_6H_4$-4-NO_2)(PPh_3)$_2$] (X = F, Cl, Br, I) and found the $\Delta\nu$(CO) = 17 cm^{-1}. The magnitude of $\Delta\nu$(CO) is identical within experimental error ($\pm$4 cm^{-1}) to that observed for **2a**–**d**. It is clear that the non-conventional *cis*-push–pull effect, Chart 1, appears to be too small in magnitude to be effectively probed using ν(CO) values although it is amenable to measurement by ^{13}C NMR spectroscopy [2].

2.2. Synthesis and characterization of [HgBr{η^2-C_6H_4-2-CH($O_2C_2H_4$)}] (4)

During the preparation of **1** [HgBr{η^2-C_6H_4-2-CH($O_2C_2H_4$)}] (**4**) was isolated as a side product. It can be readily prepared in high yield on treatment of BrMg-(C_6H_4-2-$CHO_2C_2H_4$) [4] with 1 equiv. of $HgBr_2$. Compound **4** has been characterized by elemental analysis Table 1, ^{1}H NMR Table 2 and ^{13}C–{^{1}H}NMR spectroscopy Table 3. A suitable crystal for an X-ray diffraction study was obtained on recrystallization from hot ethanol, see Table 4 for data collection and processing parameters and Fig. 6 for an ORTEP [20] representation showing the atomic numbering scheme with selected bond lengths (Å) and angles (°). The most noticeable feature of this structure is the pyramidal nature of the coordinated oxygen atom. Theoretical calculations (B3LYP using the LanL2DZ basis set) [13] on the model compounds [HgBr(C_6H_4-2-CH_2EH)] (**5a**,**b**), Figs. 7 and 8, predict, as for the ruthenium compounds **3a**,**b**, a planar oxygen atom, which differs from the crystallographically determined structure, and pyramidal sulfur. See Supplementary material for calculated bond lengths (Å) and angles (°).

Inspection of the extended structure for **4**, Fig. 9, shows that the coordinated acetal–oxygen atom bridges two mercury centres, 2.816(4) and 2.882(5) Å respectively, and has a pseudo-tetrahedral coordination geometry.

Additionally the coordination number at the mercury centre expands to six through two additional long Hg···Br interactions at 3.652(5) and 3.395(5) Å respectively which are comfortably within the sum of the van der Waals radii [4,21]. The differences between the calculated and solid state geometry are a pertinent reminder of the inability of this type of calculation to predict the presence of other solid state interactions and how they may influence the overall molecular geometry.

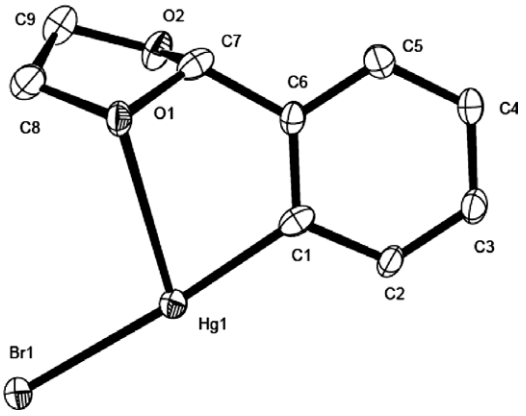

Fig. 6. ORTEP [19] representation of 4 showing the numbering scheme. Selected bond lengths (Å) and angles (°):C(1)–Hg(1) 2.041(14); Hg(1)–Br(1) 2.4475(13); O(1)–Hg(1) 2.816(12); C(7)–O(1) 1.397(17); C(7)–O(2) 1.435(14); C(8)–O(1) 1.411(16); C(9)–O(2) 1.420(16); C(1)–Hg(1)–Br(1) 175.2(4); Hg(1)–O(1)–C(7) 97.8(3); Hg(1)–O(1)–C(8) 114.1(4); C(7)–O(1)–C(8) 106.6(3).

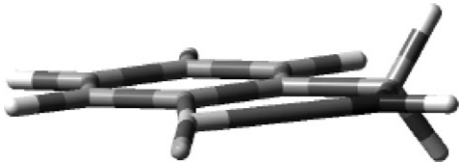

Fig. 7. SPARTAN representation of the optimized geometry of [HgBr(η^2-C_6H_4-2-CH_2OH)] (**5a**).

Fig. 8. SPARTAN representation of the optimized geometry of [HgBr(η^2-C_6H_4-2-CH_2SH)] (**5b**).

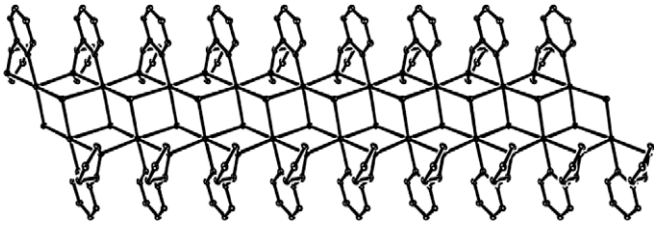

Fig. 9. ORTEP representation of the extended structure of **4.**

3. Conclusions

The preparation and structural characterization of [RuCl{η^2-*C*,*O*-C_6H_4-2-($O_2C_2H_4$)}(CO)(PPh_3)$_2$] (**2a**), along with theoretical calculations and searches of the CCDC presents an explanation of the differences in the nature of the coordination modes of ether and thioether ligands to metal centres. It also revealed, not surprisingly, that the nature and availability of the electron density at the chalcogen atom differs significantly between the oxygen and sulfur donor atoms. The electron density at the sulfur atom has the classical bunny-ear like appearance, whereas at oxygen it is more akin to a banana shape. Therefore the favoured coordination geometry for ether ligands is planar-at-oxygen and for thioether ligands is pyramidal-at-sulfur. The different coordination geometries at coordinated oxygen observed in the solid state structure of **2a** (planar and slightly pyramidal) which on a first look appear to be frozen intermediates of a classical pyramidal inversion are, in fact, frozen intermediates of a low energy pseudorotation commonly observed for five-membered rings.

4. Experimental

4.1. General comments

All solvents except alcohols were dried by refluxing over the appropriate drying agent (toluene, Na; CH_2Cl_2, P_4O_{10}; hexane, NaK) and distilled prior to use. [RuHCl(CO)(PPh_3)$_2$] [22] and Hg{*o*-C_6H_4-2-$CH(O_2C_2H_4)$}$_2$ [4], were prepared according to the literature procedures; all other chemicals were obtained from commercial sources and used as received, except for $RuCl_3 \cdot H_2O$ which was loaned by Johnson Matthey. IR spectra were recorded as nujol mulls between KBr plates on a Nicolett 5PC spectrometer, ^{1}H NMR (200.2 MHz), ^{31}P{^{1}H} (81.3 MHz) were recorded on a Bruker DPX 200 spectrometer and ^{1}H NMR (400.2 MHz), ^{31}P{^{1}H} (162.6 MHz), ^{13}C{^{1}H} NMR (100.55 MHz) were recorded on a Bruker DPX 400 spectrometer. ^{1}H and ^{13}C NMR spectra were referenced to residual C*H*Cl_3 ($\delta = 7.26$) and *C*DCl_3 ($\delta = 77.0$) and ^{31}P{^{1}H} NMR were referenced externally to 85% H_3PO_4 ($\delta = 0.0$). Elemental analyses were performed by the Microanalytical Service, Department of Chemistry, UMIST. The syntheses were carried out under a dinitrogen atmosphere using standard Schlenk techniques. Work-ups were generally carried out in the open unless otherwise stated.

4.2. Synthesis of [RuCl(CO)(η^2-$C_6H_4CHO_2C_2H_4$)(PPh_3)$_2$] (**2a**)

Caution: use of an organomercurial reagent. To [RuHCl(CO)(PPh_3)$_3$] (1.0 g, 1.04 mmol) suspended in toluene (20 mL) was added Hg{*o*-C_6H_4-2-$CH(O_2C_2H_4)$}$_2$ (0.52 g, 1.04 mmol) and the solution heated to reflux with continuous stirring under dinitrogen for 6 h. After cooling the solution was filtered through Celite® to remove Hg (caution) and the solvent removed under reduced pressure. The crude material was then extracted with hot hexane (3×25 mL) to remove PPh_3 and $C_6H_5CHO_2C_2H_4$. Recrystallization from CH_2Cl_2/EtOH afforded **2a** in good yield (0.76 g, 87%). See Table 1 for physical and analytical data.

4.3. Synthesis of [RuBr(CO)(η^2-$C_6H_4CHO_2C_2H_4$)(PPh_3)$_2$] (**2b**)

To [RuCl(CO)(η^2-$C_6H_4CHO_2C_2H_4$)(PPh_3)$_2$] (0.1 g, 0.12 mmol) dissolved in CH_2Cl_2/acetone (20 mL, 1:1) was added $AgBF_4$ (0.025 g, 0.12 mmol). After stirring for 30 min the solution was filtered through a fluted filter paper and NaBr (0.025 g, 0.24 mmol) dissolved in water (0.5 mL) was added along with enough ethanol to generate a homogeneous solution. After stirring for 30 min the solvent volume was reduced under reduced pressure affording crude **2b**. Recrystallization of the crude from CH_2Cl_2/EtOH afforded **2b** in good yield (0.95 g, 94%). See Table 1 for physical and analytical data. Compounds **2c** and **2d** were prepared in analogous fashion.

4.4. X-ray crystallography

Crystals of **2a** were grown by dissolving approximately 10 mg in 0.2 mL of CH_2Cl_2 in a glass vial (10 mm × 25 mm) and layering ether on top and leaving the mixture to stand for several days.

A suitable single crystal was coated in inert perfluoropolyether oil and mounted on a single glass wool strand of ca. 3 mm in length glued to a glass fibre. All measurements were carried out on Station 9.8. CCLRC Daresbury Laboratory, Daresbury, UK using a standard Bruker SMART charge-coupled device (CCD) 1 K area-detector diffractometer controlled using the SMART software package

version 5.054 [23]. This software was also used for indexing, cell refinement and data reduction.

The structure was solved by direct methods and subjected to full-matrix least-squares refinement on F2 using the SHELX-97 [24] program. All nonhydrogen atoms were refined with anisotropic thermal parameters, while hydrogen atoms were fixed in idealized positions. Crystal data and details of the refinement are presented in Table 4 and a PLUTON [10] generated image of the asymmetric unit is displayed in Fig. 1.

The asymmetric unit consists of four complex molecules and a diethylether solvate. Although the structure contains cavities that are sufficiently large to accommodate more diethylether molecules there is no evidence of them in the difference maps, although a highly disordered second solvate molecule cannot be ruled out. A packing diagram is included in Supplementary material.

The current crystal structure determination was hampered by two types of crystal imperfection: (i) The beta angle is almost exactly 90° so it is not surprising that twinning has occurred. Although the twin command TWIN $-1\,0\,0\,0\,1\,0\,0\,0\,1$ defines the twin plane as the *bc* plane, monoclinic symmetry means that the *ab* plane, *a*-axis or *b*-axis are equally plausible twinning symmetry elements. The ratio of the main crystal to its twin as refined with the BASF command is 0.6022(8):0.3978(8).

(ii) A non-crystallographic *a*-glide $(0.5 + x, y, 0.446 - z)$ relates the enantiomeric pairs in each 4-molecule cluster and is the most probable explanation for Ru ghost peaks that are observed at $(x, y, z + 0.11)$ with site occupancies of 3% of the main Ru atoms. The crystallographic screw axis $(-x, 0.5 + y, 0.5 - z)$, which relates the clusters down *b* can be combined with the non-crystallographic *a*-glide $(0.5 + x, y, 0.446 - z)$ to create a non-crystallographic "diagonal" glide $(0.5 - x, 0.5 + y, 0.054 + z)$. Although the non-crystallographic "diagonal" glide is not applied a second time as the mirror is returned to its original position by the crystallographic 2_1, it is clearly an acceptable packing option. If the non-crystallographic "diagonal" glide operation is applied twice a pure translation results, $(x, 1 + y, 0.108 + z)$ c.f. $(x, y, 1 + z)$ for a double application of the 2_1 axis. Therefore occasional application of the non-crystallographic operation as opposed to the crystallographic 2_1 would lead to ghost Ru peaks displaced from the main Ru atoms by 0.108 down z^*. This also suggests the possibility of a second polymorph, in which the "diagonal" glide becomes the main operation. This would change the shape of the unit cell $a' = a$, and $c' = c$ but $\alpha' = 180 - a\tan b/0.108c$ and $b' = b/\sin\ \alpha'$. This would lead to the glide operation reflecting in the $b'c'$ plane and translating down b'. Conversion to the conventional *ac* plane reflection and translation down *c* is achieved via. $a'' = c' = c = 41.8390$; $b'' = a' = a = 10.7814$; $c'' = b' = b/\sin\ \alpha' = b/\sin\ \beta'' = 36.448$; $\beta'' = \alpha' = 180 - a\tan\ b/0.108c = 97.12$. A second polymorph has been observed, which has crystallized in space group $P2_1/c$ with unit cell dimensions $a = 41.9326$, $b = 10.8103$, $c = 36.5987$ and $\beta = 97.781$. The quality of these crystals was extremely poor and it was only possible to collect data to 20° theta for Mo radiation. Nevertheless the 4-molecule cluster seen in the current structure and the packing anticipated above appear to be borne out.

Crystals of **4** were grown by a slow cooling of a hot 50 °C saturated solution. A suitable single crystal was attached to a glass fibre using inert perfluoropolyether oil. The X-ray diffraction data were collected on a Nonius Kappa CCD 4-circle diffractometer controlled using KappaCCD Server Software [25] and COLLECT [26]. Final cell refinement and data reduction were carried out using DENZO and SCALEPACK from the HKLf suite of programmes [27].

The structure was solved by direct methods and subjected to full-matrix least-squares refinement on F^2 using the SHELX-97 [24] program. All nonhydrogen atoms were refined with anisotropic thermal parameters, while hydrogen atoms were fixed in idealized positions. Crystal data and details of the refinement are presented in Table 4 and a molecular image, generated using ORTEP 3 for Windows [19], is displayed in Fig. 6.

Acknowledgements

K.R.F. thanks the EPSRC National Crystallographic service, University of Southampton for a preliminary data collection on **2a** and Johnson Matthey for the loan of $RuCl_3 \cdot H_2O$.

Appendix A. Supplementary material

CCDC 633950, 633951and 633952 contain the supplementary crystallographic data for **2a** (Synchrotron), **4** and **2a** (KappaCCD). These data can be obtained free of charge via http://www.ccdc.cam.ac.uk/conts/retrieving.html, or from the Cambridge Crystallographic Data Centre, 12 Union Road, Cambridge CB2 1EZ, UK; fax: (+44) 1223-336-033; or e-mail: deposit@ccdc.cam.ac.uk. Histogram representations of the CCDC searches, packing diagrams for **2a**, and calculated bond lengths (Å) and angles (°) for **3a**–**b** and **5a**–**b** are available. Supplementary data associated with this article can be found, in the online version, at doi:10.1016/j.jorganchem.2007.02.029.

References

[1] (a) W.I. Cross, K.R. Flower, R.G. Pritchard, J. Organomet. Chem. 601 (2000) 164;
(b) K.R. Flower, R.G. Pritchard, J. Organomet. Chem. 620 (2001) 60.
[2] K.R. Flower, V.J. Howard, R.G. Pritchard, J.E. Warren, Organometallics 21 (2002) 1184.
[3] K.G. Caulton, New J. Chem. 18 (1994) 25, and references cited therein.
[4] K.R. Flower, V.J. Howard, S. Naguthney, R.G. Pritchard, J.E. Warren, A.T. McGown, Inorg. Chem. 41 (2002) 1907.
[5] (a) P.J. Heard, P.M. King, P. Sroisuwan, N. Kaltsoyannis, Polyhedron 22 (2003) 3371;
(b) P.J. Heard, P.M. King, D.A. Tocher, J. Chem. Soc., Dalton Trans. (2000) 1769;

(c) P.J. Heard, P.M. King, A.D. Bain, P. Hazendonk, D.A. Tocher, J. Chem. Soc., Dalton Trans. (1999) 4495.
[6] (a) Recent papers: J. Andrieu, J.-M. Camus, P. Richard, R. Poli, L. Gonsalvi, F. Vizza, M. Peruzzini, Eur. J. Inorg. Chem. (2006) 51;
(b) D.B. Grotjahn, Y. Gong, L. Zakharov, J.A. Golen, A.L. Rheingold, J. Am. Chem. Soc. 128 (2006) 438;
(c) R. Wang, B. Twamley, J.M. Shreeve, J. Org. Chem. 71 (2006) 426;
(d) N. Fuchs, M. D'Augustin, M. Humam, A. Alexakis, R. Taras, G.A. Gladiali, Tetrahedron: Asymmetry 16 (2005) 3143;
(e) S.L. Parisel, L.A. Adrio, A.A. Pereira, M.M. Perez, J.M. Vila, K.K. Hii, Tetrahedron 61 (2005) 9822;
(f) G. Kohl, R. Rudolph, H. Pritzkow, M. Enders, Organometallics 24 (2005) 4774;
(g) D. Gareau, C. Sui-Seng, L.F. Groux, F. Brisse, D. Zargarian, Organometallics 24 (2005) 4003;
(h) W.-M. Dai, Y. Zhang, Tetrahedron Lett. 46 (2005) 1377;
(i) J. Heinicke, M. Koehler, N. Peulecke, M.K. Kindermann, W. Keim, M. Koeckerling, Organometallics 24 (2005) 344;
(j) A. Friedrich, U. Radius, Eur. J. Inorg. Chem. (2004) 4300;
(k) R.J. Van Haaren, H. Oevering, P.C.J. Kamer, K. Goubitz, J. Fraanje, P.W.N.M. Van Leeuwen, G.P.F. Van Strijdonck, J. Organomet. Chem. 689 (2004) 3800;
(l) A. Caballero, F.A. Jalon, B.R. Manzano, P.-M. Gustavo, M. Mercedes, F.J. Poblete, M. Maestro, Organometallics 23 (2004) 5694;
(m) Reviews:H.J. Werner, Chem. Soc., Dalton Trans. (2000) 3829;
(n) P. Laurent, N. Le Bris, H. des Abbayes, Trends Organomet. Chem. 4 (2002) 31;
(o) U. Schubert, J. Pfeiffer, F. Stohr, D. Sturmayr, S.J. Thompson, J. Organomet. Chem. 646 (2002) 53;
(p) P. Braunstein, F. Naud, Angew. Chem., Int. Ed. Engl. 40 (2001) 680;
(q) C. Muller, D. Vos, P.J. Jutzi, J. Organomet.Chem. 600 (2000) 127;
(r) G. Lavigne, Eur. J. Inorg. Chem. (1999) 917;
(s) C.S. Slone, D.A. Weinberger, C.A. Mirkin, Prog. Inorg. Chem. 48 (1999) 233.
[7] J. Vicente, J.-A. Abad, F.S. Hernández-Mata, B. Rink, P.G. Jones, M.C.R. de Arellano, Organometallics 23 (2004) 1292.
[8] (a) K. Ferre, G. Poignant, L. Toupet, V. Guerchais, J. Organomet. Chem. 629 (2001) 19;
(b) J.J. Daly, F. Sanz, R.P.A. Sneeden, Raymond H.H. Zeiss, Helv. Chim. Acta 57 (1974) 1863.
[9] W.R. Roper, L.J. Wright, J. Organomet. Chem. 142 (1977) C1.
[10] A.L. Spek, Acta Crystallogr., Sect. A 46 (1990) C34.
[11] D.G. Lister, J.N. MacDonald, N.L. Owen, Internal Rotation and Inversion, Academic Press, London, New York, San Francisco, 1978, pp. 171–196 (Chapter 7).
[12] (a) K.M. Williams, D.J. Chapman, S.R. Maney, C. Haare, J. Inorg. Biochem. 99 (2005) 2119;
(b) G. Tresoldi, L. Baradello, S. Lanza, P. Cardiano, Eur. J. Inorg. Chem. (2005) 2422;
(c) M. Herberhold, J. Liu, W. Milius, O. Tok, B. Wrackmeyer, Z. Anorg. Allg. Chem. 630 (2004) 2438;
(d) L. Zhong, X. Wen, T.M. Rabinowitz, B.S. Russell, E.F. Karan, K.L. Bren, Proc. Natl. Acad. Sci. USA 101 (2004) 8637;
(e) D. Balcells, F. Maseras, N. Khiar, Org. Lett. 6 (2004) 2197;
(f) M. Bassetti, A. Capone, M. Salamone, Organometallics 23 (2004) 247;
(g) G. Tresoldi, S.L. Schiavo, S. Lanza, P. Cardiano, Eur. J. Inorg. Chem. (2002) 181;
(h) J.W. Cubbage, W.S. Jenks, J. Phys. Chem. A 105 (2001) 10588;
(i) J. Dupont, A.S. Gruber, G.S. Fonseca, A.L. Monteiro, G. Ebeling, R.A. Burrow, Organometallics 20 (2001) 171;
(j) S. Toyota, Rev. Heteroatom Chem. 21 (1999) 139;
(k) H. Torrens, Coord. Chem. Rev. 196 (2000) 331;
(l) E.W. Abel, K.G. Orrell, M.C. Poole, V. Sik, Polyhedron 18 (1999) 1345;
(m) J.R. Ascenso, M.de D. Carvalho, A.R. Dias, C.C. Romao, M.J. Calhorda, L.F. Veiros, J. Organomet. Chem. 470 (1994) 147;
(n) E.W. Abel, P.J. Heard, K.G. Orrell, M.B. Hursthouse, M.A. Mazid, J. Chem. Soc., Dalton Trans. (1993) 3795;
(o) M.L.H. Green, D.K.P. Ng, J. Chem. Soc., Dalton Trans. (1993) 11;
(p) E.W. Abel, K.G. Orrell, H. Rahoo, V. Sik, J. Organomet. Chem. 441 (1992) 255;
(q) E.W. Abel, J.C. Dormer, D. Ellis, K.G. Orrell, V. Sik, M.B. Hursthouse, M.A. Mazid, J. Chem. Soc., Dalton Trans. (1992) 1073;
(r) M.Y. Darensbourg, M. Pala, S.A. Houliston, K.P. Kidwell, D. Spencer, S.S. Chojnacki, J.H. Reibenspies, Inorg. Chem. 31 (1992) 1487;
(s) E.W. Abel, D. Ellis, K.G. Orrell, V. Sik, Polyhedron 10 (1991) 1603;
(t) A. Gryff-Keller, P. Szczecinski, H. Koziel, Magn. Res. Chem. 26 (1988) 468;
(u) E.W. Abel, S.K. Bhargara, K.G. Orell, Prog. Inorg. Chem. 32 (1984) 1.
[13] F.H. Allen, J.E. Davies, O.J. Johnson, O. Kennard, C.F. Macrae, G.F. Mitchell, J.M. Smith, D. Watson, J. Chem. Inf. Comput. Sci. 31 (1991) 187.
[14] GAUSSIAN 03, Revision C.02, Gaussian, Inc., Wallingford, CT, 2004.
[15] SPARTAN O4, Wavefunction Inc., 18401 Von Karman Avenue, Suite 370, Irvine, CA 92612, USA.
[16] C. Gourlaouen, J.-P. Piquemal, T. Saue, O. Parisel, J. Comput. Chem. 27 (2006) 142.
[17] (a) J.E. Kilpatrick, E.S. Pitzer, J. Spitzer, J. Am. Chem. Soc. 69 (1947) 2483;
(b) J.D. Dunitz, X-ray analysis and the structures of organic molecules, Cornell University Press, Ithaca, 1979, p. 425;
(c) J. Casanovas, A.M. Namba, R. Da Silva, C. Aleman, Bioorg. Chem. 33 (2005) 484;
(d) A. Wu, D. Cremer, A.A. Auer, J. Gauss, J. Phys. Chem. A 106 (2002) 657;
(e) S.J. Han, Y.K. Kang, Theochem 369 (1996) 157;
(f) Z. Dzakula, M.L. DeRider, J.L. Markley, J. Am. Chem. Soc. 118 (1996) 12796;
(g) S.J. Han, Y.K. Kang, Theochem 362 (1996) 243;
(h) M. Tomimoto, N. Go, J. Phys. Chem. 99 (1995) 563;
(i) C.J. Marzec, L.A. Day, J. Biomol. Struct. Dynam. 10 (1993) 1091;
(j) N. Juranic, S.R. Niketic, K. Andjelkovic, I. Juranic, J. Mol. Struct. 271 (1992) 209;
(k) R.L. Rosas, C. Cooper, J. Laane, J. Phys. Chem. 94 (1990) 1830;
(l) F.A.A.M. De Leeuw, P.N. Van Kampen, C. Altona, E. Diez, A.L. Esteban, J. Mol. Struct. 125 (1984) 67;
(m) P. Herzyk, A. Rabczenko, J. Chem. Soc., Perkin Trans. 2 (1983) 213;
(n) E. Abillon, Biophys. Struct. Mech. 9 (1982) 11;
(o) S.T. Rao, E. Westhof, M. Sundaralingam, Acta Crystallogr., Sect. A A37 (1981) 421;
(p) E. Westhof, M. Sundaralingam, J. Am. Chem. Soc. 102 (1980) 1493;
(q) D. Cremer, J.A. Pople, J. Am. Chem. Soc. 97 (1975) 1358.
[18] K.R. Flower, R.G. Pritchard, J.E. Warren, Eur. J. Inorg. Chem. (2003) 1929.
[19] K. Fagnou, M. Lautens, Angew. Chem., Int. Ed. Engl. 41 (2001) 26.
[20] L.J. Farrugia, J. Appl. Crystallogr. 30 (1997) 565.
[21] A. Bondi, J. Phys. Chem. 68 (1964) 441.
[22] N. Ahmad, J.J. Levison, S.D. Robinson, M.F. Uttley, Inorg. Synth. 15 (1974) 45.

[23] SMART: Area-Detector Software Package, Bruker, Madison, WI, 1998.
[24] G.M. Sheldrick, Programs for Crystal Structure Analysis (release 97-2), University of Göttingen, 1998.
[25] KappaCCD Server Software: Windows 3.11 Version. B.V. Nonius, Delft, The Netherlands (1997).
[26] COLLECT. B.V. Nonius Delft, The Netherlands, 1998.
[27] HKL DENZO HKL SCALEPACK: Z. Otwinowski, W. Minor, Methods in enzymology, in: C.W. CarterJr., R.M. Sweet (Eds.), Macromolecular Crystallography, Part A, vol. 276, Academic Press, New York, 1997, pp. 307–326.